Modified Parker weights for super short scan cone beam CT

Dirk Schäfer, Peter van de Haar, Michael Grass

***Abstract*— Circular cone beam CT (CBCT) acquisitions with less than 180° plus fan angle are desired for practical reasons in the interventional setup. Strong shading artefacts are present with standard FDK reconstruction even for voxels with 180° coverage. The use of modified Parker weights has been proposed to correctly handle redundant data and correct for shading in the limited angle areas. However, this results in discontinuous weighting functions leading to streak artefacts in the FDK reconstruction. We propose to combine the modified Parker weights with a filtered back-projection (FBP) algorithm capable of handling redundancy weights after filtering. Improved image quality is shown for this approach in terms of visual appearance and quantitative measures.**

I. Introduction

Circular short scan acquisitions with trajectories covering $180° +$ fan-angle are wide-spread in interventional use with C-arm systems. Due to timing, workflow and space constraints even shorter trajectories are desired from a practical perspective. The standard FDK-reconstruction fails in these super-short scan (limited angle) scenarios without applying Parker weights (see Fig. 5B) or with (modified) Parker weights (Fig. 7B). Iterative methods have been investigated for limited angle acquisitions [8] also with dedicated anisotropic regularization [1] to mitigate streaks caused by the missing projection angles. For interventional use we concentrate on FBP methods due to reconstruction time constraints.

Noo et al. [5] proposed a FBP algorithm for circular arc scan acquisitions that is capable to exactly reconstruct those voxels that have been seen on 180° including disconnected arcs or super short scan arcs. Riess et al. [7] considered the mitigation of artefacts for the voxels not satisfying the 180° condition by introducing a modified version of the well known Parker weights. They applied correct redundancy weights for rays measured twice and over-weighted rays that are close to the missing rays to correct for shading artefacts. The modified Parker weights result in discontinuous weighting functions in central detector areas. The subsequent ramp filtering of the FDK reconstruction leads to streak artefacts (see Fig. 7B). Riess proposed heuristic low-pass filtering to mitigate these streaks, but did not investigate this thoroughly. In this paper, we propose to combine the modified Parker weights with the Noo reconstruction for super short scans and investigate the performance compared to FDK reconstruction with low-pass filtering of the modified weights.

DS and MG are with Philips Research Hamburg, Röntgenstraße 24–26, 22335 Hamburg, Germany. PvdH is with Philips Healthcare, Veenpluis 6, 5684 PC Best, The Netherlands. corresponding author: dirk.schaefer@philips.com

II. Methods

A. Parker Weights

A schematic view of the acquisition geometry is shown in Fig. 1. The source $\mathbf{s}(\lambda)$ and the planar detector with N_v rows and N_u columns are rotated around the y-axis along a circular arc with N_λ projections along the path length Λ. The distance from the source to the detector origin $\mathbf{d}(\lambda)$ is denoted D and the distance to the the iso-center $\mathbf{i}$ on the rotation axis is R. The normalized vector $\hat{\mathbf{c}}(\lambda)$ points from $\mathbf{d}(\lambda)$ to the iso-center, and $\hat{\mathbf{e}}(u,v,\lambda)$ is the unit vector from $\mathbf{s}(\lambda)$ to the detector element $\mathbf{d}(u,v,\lambda)$. The corresponding length is denoted by $\overline{SE}$. The v-axis is parallel to the rotational axis and the u-axis is parallel to the trajectory tangent vector. The cone beam line integral projection data of the object f_0 is denoted by $g(u,v,\lambda)$:

$$g(u,v,\lambda) \quad = \quad \int_0^\infty f_0(\mathbf{s}(\lambda) + l\hat{\mathbf{e}}(u,v,\lambda))\mathrm{d}l.$$

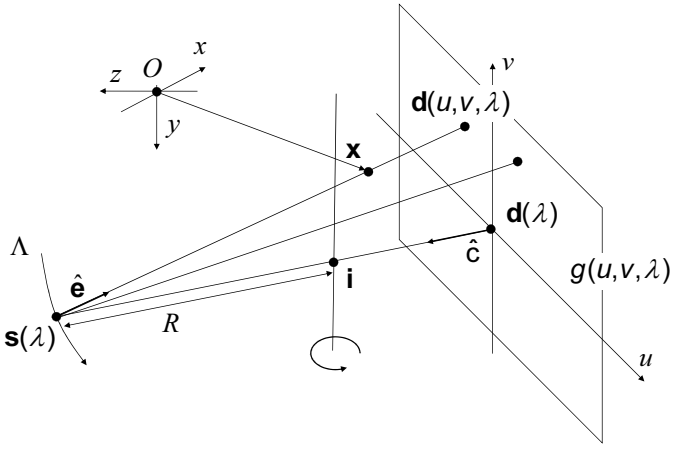

Fig. 1. Geometry for circular X-ray tomography.

Redundant rays occur in the mid-plane satisfying:

$$\bar{g}(\alpha,0,\beta) = \bar{g}(-\alpha,0,\beta+2\alpha+\pi), \tag{1}$$

where the fan angle α of a specific ray u is given by $\alpha(u) = \mathrm{atan}(u/D)$ and the source angle by $\beta(\lambda) = \lambda/R$. The bar denotes the change of variables $(u,v,\lambda) \rightarrow (\alpha,v,\beta)$.

Parker-Silver weights [4][9] handle redundant and complementary rays with non-vanishing cone-angle:

$$\bar{w}(\alpha,\beta) =$$

$$\begin{cases} \sin^2\left(\frac{\pi}{4}\frac{\beta}{\gamma-\alpha}\right) & 0 \leq \beta < 2\gamma-2\alpha, \\ 1 & 2\gamma-2\alpha \leq \beta \leq \pi-2\alpha, \\ \sin^2\left(\frac{\pi}{4}\frac{\pi+2\gamma-\beta}{\gamma+\alpha}\right) & \pi-2\alpha < \beta \leq \pi+2\gamma, \end{cases} \tag{2}$$

DOI: 10.12059/Fully3D.2017-11-3106003

where the redundant half angle γ is calculated from the detector fan angle 2δ and the overscan angle 2ϵ: $\gamma = \delta + \epsilon$. An illustration is given in Fig.2A (adapted from [10]).
In the case of a super short scan, e.g. 180 degrees, some measured rays are redundant and some needed rays are missing. Riess et al. [7] proposed modified weights w_m that sum up redundant rays to unity, whereas those rays close to the missing rays receive weights larger than unity:

$$\bar{w}_m(\alpha,\beta) = \begin{cases} \sin^2\left(\frac{\pi}{4}\frac{\beta}{\gamma-\alpha}\right) & 0 \le \beta < 2\gamma - 2\alpha, \\ 2 - \sin^2\left(\frac{\pi}{4}\frac{\beta}{\gamma-\alpha}\right) & 0 \le \beta < -2\gamma + 2\alpha, \\ \sin^2\left(\frac{\pi}{4}\frac{\pi+2\gamma-\beta}{\gamma+\alpha}\right) & \pi - 2\alpha < \beta \le \pi + 2\gamma, \\ 2 - \sin^2\left(\frac{\pi}{4}\frac{\pi+2\gamma-\beta}{\gamma+\alpha}\right) & \pi + 2\gamma + 2\alpha < \beta \le \pi + 2\gamma, \end{cases} \quad (3)$$

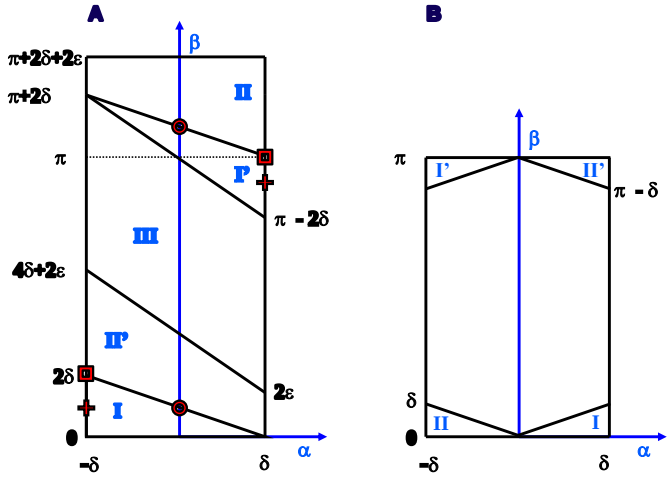

Fig. 2. A: Parker sinogram in fan-beam geometry. The areas I / I' are redundant and II / II'. Identical marker highlight selected redundant rays.
B: fan-beam sinogram of an 180° acquisition. The areas II / II' are redundant, whereas the the areas I / I' receive weights > 1.0.

The modified weights w_m can nicely compensate for the intensity drop in the region of missing rays, but cannot correct for limited angle artefacts. Furthermore, they introduce new streak artefacts with standard FDK [2] reconstruction due to a non-continuous jump in the weighting function for the first and last projection.
Riess et. al [7] proposed to mitigate this by heuristic low-pass (LP) filtering of the weights in the first and last projection, but did not mention any parameters used.
We propose to parametrize the low-pass filtering of the modified Parker weights by the standard deviation σ of a Gaussian kernel and the angular range Θ of the trajectory, where low-pass filtering is applied:

$$w_{m/LP}(u,\lambda;\sigma,\Theta) = \begin{cases} w_m(u,\lambda) & \Theta < \beta(\lambda) < \pi + 2\gamma - \Theta, \\ w_m(u,\lambda) * G_\sigma(u) & \text{else.} \end{cases} \quad (4)$$

The modified and additionally low-pass filtered Parker weights are computed for a 180 degree acquisition with 512 pixels of a flat detector corresponding to a fan angle of $2\delta = 18°$. The original and three different convolution results ($\sigma = 10, 20, 30$ pixels) are shown for $\beta = 0°$ and $\beta = 2°$ in Figs. 3 and 4, respectively. However, it has to be noted that this heuristic filtering destroys the normalization of the weights and may introduce new inconsistencies and related shading artefacts.

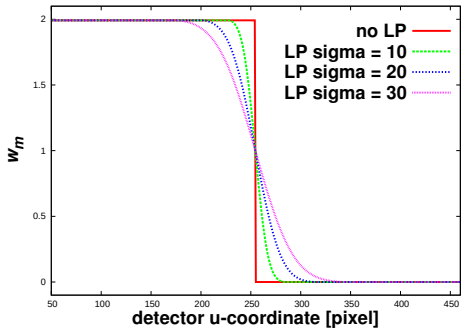

Fig. 3. Modified Parker weights w_m and low-pass filtered versions $w_{m/LP}(u,\lambda;\sigma,\Theta)$ for $\beta = 0°$ of a 180° trajectory.

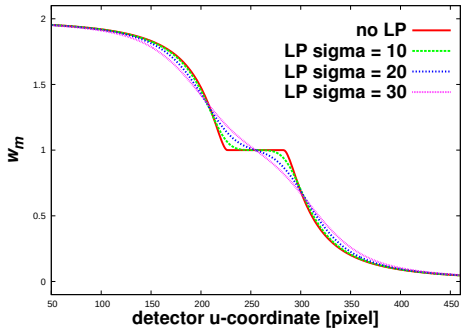

Fig. 4. Modified Parker weights w_m and low-pass filtered versions $w_{m/LP}(u,\lambda;\sigma,\Theta)$ for $\beta = 2°$ of a 180° trajectory.

B. Reconstruction

The standard FDK reconstruction is given by [2]:

$$f_{FDK}(\mathbf{x}) = \int_\Lambda \left(\frac{R}{R-(\mathbf{x}-\mathbf{i})\cdot\hat{\mathbf{c}}}\right)^2 \int_{-\infty}^{\infty} \frac{D}{\overline{SE}(\mathbf{x})} w(u',\lambda)\, g(u',v,\lambda)\, h_r(u-u')\, \mathrm{d}u'\, 1/R\, \mathrm{d}\lambda,$$

where h_r is the ramp filter and $w(u',\lambda)$ are the redundancy weights which are replaced by the modified weights of Eq.3. Instead of using the FDK algorithm with redundancy weighting before the filtering, which introduces streak artifacts, we

propose to combine the modified Parker weights with the algorithm presented by Noo et al [5], [6]:

$$f_{Noo}(\mathbf{x}) = \frac{1}{2\pi}\int_{\Lambda}\frac{w(u,\lambda)}{R-(\mathbf{x}-\mathbf{i})\cdot\hat{\mathbf{c}}}\int_{-\infty}^{\infty}\frac{D}{\overline{SE}(\mathbf{x})} g_d(u',v,\lambda)\; h_H(u-u')\;\mathrm{d}u'\;(1/R)\,\mathrm{d}\lambda, \quad (5)$$

$$\text{with}\quad h_H(\rho) = -\int_{-\infty}^{\infty} i\;\mathrm{sgn}(P)e^{j2\pi\rho P}\,\mathrm{d}P,$$

$$\text{and}\quad g_d(u,v,\lambda) = \left(\frac{\partial g}{\partial\lambda}+\frac{\partial g}{\partial u}\frac{\partial u}{\partial\lambda}+\frac{\partial g}{\partial v}\frac{\partial v}{\partial\lambda}\right)(u,v,\lambda).$$

Due to the differentiation in parallel beam geometry, the redundancy weight can be applied *after* the filtering step. This avoids the problems of applying the high-pass ramp filter to a steep weighting function w_m.

III. Results

A simulation has been performed using a flat detector of $380\times 294\,\mathrm{mm}^2$ with 512×396 pixels. Source and detector rotate on a circular arc with $R = 805$ mm and $D = 1195$ mm, which leads to a detector fan angle of $2\delta \approx 18°$. A reference trajectory for a complete short scan of 200° and a super-short scan of

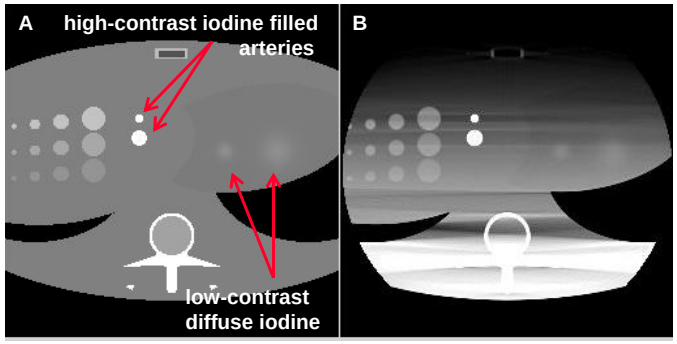

Fig. 5. Transaxial central slice through the voxelated phantom (left), and the FDK-reconstruction with $w(u,\lambda)\equiv 1$, L/W 0/600 HU.

Reconstructions of the FDK short scan reference, a Noo-reconstruction with modified weights and FDK reconstructions with modified and low-pass filtered Parker weights are shown in Fig. 7. The source travels on a half circle below the horizontal mid axis. This can easily be seen by the limited angle artifacts especially present around the sternum and the high contrast arteries. The suppression of these artefacts is beyond the scope of this paper.

The FDK-recon with modified weights w_m (Fig. 7B) is able to restore the object in the lower part inside the convex hull of the trajectory and to correct for the dark shading in the upper half compared to Fig. 5B. However, the very prominent bright streak due to the step in the weights w_m spoils the image. The FDK reconstructions with the low-pass filtered modified weights $w_{m/LP}$ reduce the horizontal streak effectively, but also introduce new shading and streak artefacts.

According to the visual inspection the best setting with low-pass filtered weights is obtained with $w_{m/LP} = w_m(u,\lambda;\sigma = 30,\Theta = 10°)$ in (Fig. 7J), but slight shadings are introduced around the spine and the contrast inserts.

The Noo-reconstruction with modified weights w_m gives ideal reconstruction in the lower half, the expected limited angle artefacts in the upper half and no additional shading or streaks. Similar results are obtained for non-central slices which are omitted for sake of brevity.

In order to check this observation quantitatively the Mean Structural SIMilarity (MSSIM) of a 2D slice y with respect to a reference x is computed [11]:

$$SSIM(x_j,y_j) = \frac{(2\mu_{x_j}\mu_{y_j}+C_1)(2\varsigma_{x_jy_j}+C_2)}{(\mu_{x_j}^2+\mu_{y_j}^2+C_1)(\varsigma_{x_j}^2+\varsigma_{y_j}^2+C_2)}$$

$$MSSIM(x,y) = \sum_{j=1}^{M} SSIM(x_j,y_j)$$

with: $C_1 = (0.01\,L)^2, C_2 = (0.03\,L)^2$,

where L is the value range of the first argument x.

The SSIM is calculated for every location x_j, y_j, where μ_{x_j} denotes the local mean, ς_{x_j} the local standard deviation and $\varsigma_{x_jy_j}$ the local covariance. We computed the SSIM in 15×15 windows for all M voxels in the field.of-view in the central slice.

The MSSIM for the reconstructed slices shown in Fig. 7 is shown in Fig. 6. The quantitative MSSIM measure supports the visual assessment: The larger low-pass kernels $\sigma = 20, 30$ give better results, when filtering 2° or 10° at the ends of the trajectory. The MSSIM value for the Noo-reconstruction of 0.91 is given as reference line, which is clearly outperforming the other methods.

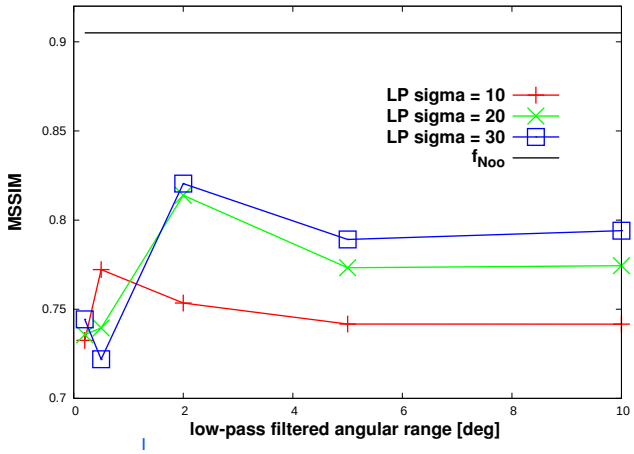

Fig. 6. MSSIM for reconstructions.

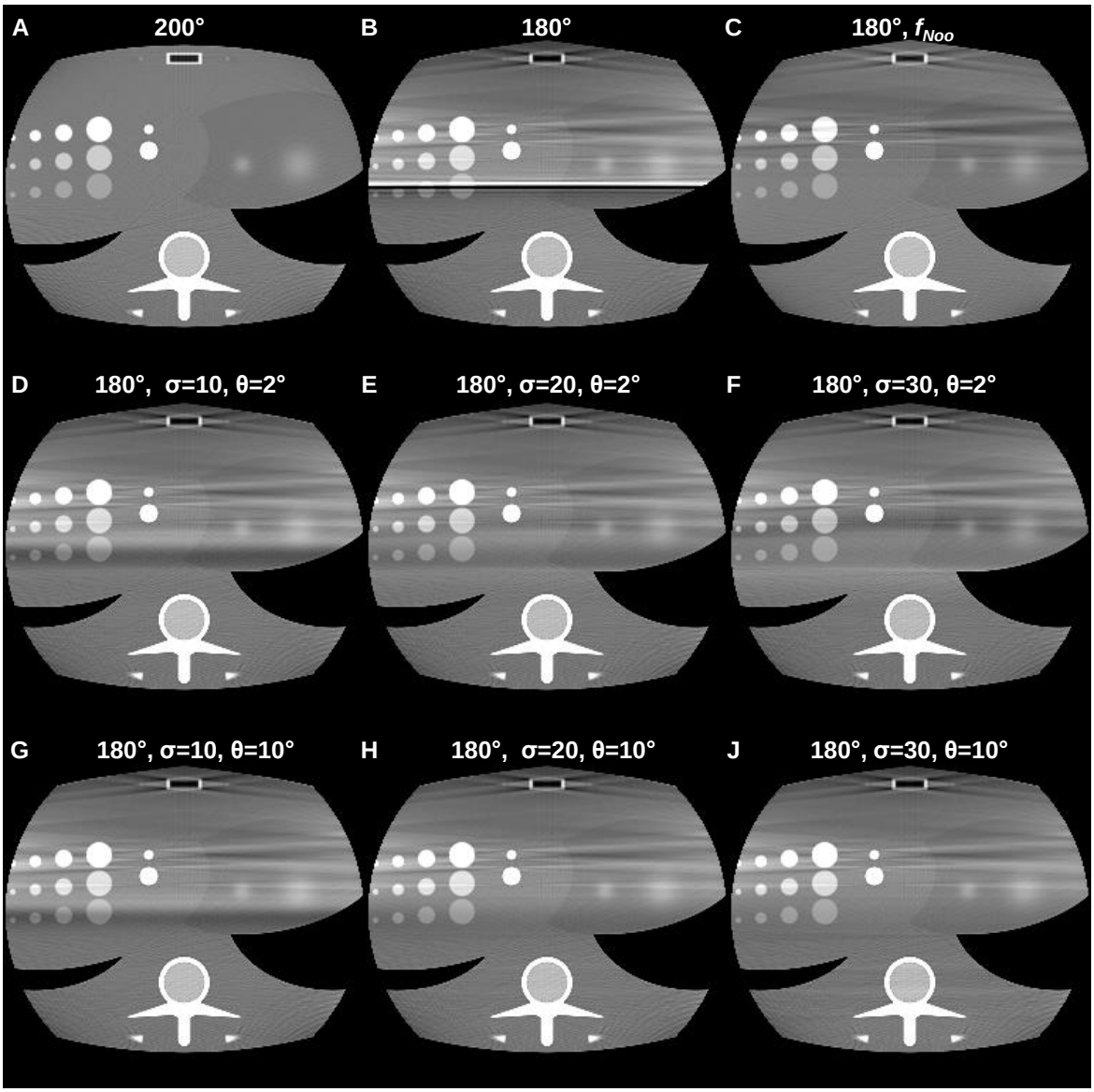

Fig. 7. Central transaxial slice through the simulated phantom for different reconstructions, L/W 0/300 HU, 1 mm slice thickness. The source trajectory is a 180° half circle around the lower part of the phantom. FDK 200° short scan reference (A), super short scan with w_m and FDK-recon (B), super short scan with w_m and Noo-recon (C), super short scan with $w_{m/LP}$ and FDK-recon (D-J).

IV. Summary and Conclusion

The Noo reconstruction with the modified Parker weights cleans up the areas with redundantly measured data and removes shading artefacts in the limited angle reconstruction area. It outperforms the investigated FDK reconstructions with modified Parker weights and the heuristically smoothed weights.

References

[1] Z. Chen, X. Jin, L. Li, and G. Wang, "A limited-angle ct reconstruction method based on anisotropic tv minimization," Physics in Medicine and Biology, Vol. 58(7), 2119, 2013.

[2] L. Feldkamp, et al., "Practical cone-beam algorithm," J. Opt. Soc. Am. A **1**, 612-619, 1984.

[3] http://www.imp.uni-erlangen.de/phantoms/thorax/thorax.htm

[4] D. Parker, "Optimal short scan convolution reconstruction for fan beam CT," Med. Phys. **9**, 254-257, 1982.

[5] F. Noo, M. Defrise, R. Clackdoyle, H. Kudo, "Image reconstruction from fan-beam projections on less than a short scan," Phys. Med. Biol. Vol. 47, 2525–2546, 2002.

[6] F. Noo, S. Hoppe, F. Dennerlein, G. Lauritsch, J. Hornegger, "A new scheme for view-dependent data differentiation in fan-beam and cone-beam computed tomography," Phys. Med. Biol. Vol. 52, pp. 5393–5414, 2007.

[7] C. Riess, M. Berger, H. Wu, M. Manhart, R. Fahrig and A. Maier, "TV or not TV? That is the Question," Fully3D meeting, p. 341-344, 2013.

[8] EY. Sidky, C. Kao, X. Pan, "Accurate image reconstruction from few-views and limited-angle data in divergent-beam CT," J X-Ray Sci Technol., Vol. 14, pp. 1–21, 2006.

[9] MD. Silver, "A method for including redundant data in computed tomography," Med. Phys., Vol. 27, pp. 773–774, 2000.

[10] S. Wesarg, M. Ebert, T. Bortfeld, "Parker weights revisited," Med. Phys., Vol. 29, pp. 372-378, 2002.

[11] Z. Wang, AC. Bovik, HR. Sheikh, and EP. Simoncelli, "Image Qualifty Assessment: From Error Visibility to Structural Similarity," IEEE Transactions on Image Processing, Vol. 13(4), pp. 600–612, 2004.